Wang *et al. BMC Cardiovascular Disorders* (2025) 25:48
https://doi.org/10.1186/s12872-025-04499-w

BMC Cardiovascular Disorders

RESEARCH

Open Access

Feasibility analysis of non-electrocardiogram-triggered chest low-dose computed tomography using a kV-independent reconstruction algorithm for predicting cardiovascular disease risk in patients receiving maintenance hemodialysis

Xiangming Wang[1†], Ao Liu[1†], Yan Zhao[2], Xianbo Yu[3], Yushuo Cao[1], Min Li[1], Jing Liu[1], Yu Du[1] and Li Yang[1*]

Abstract

Objectives This study aimed to evaluate the feasibility and accuracy of non-electrocardiogram (ECG)-triggered chest low-dose computed tomography (LDCT) with a kV-independent reconstruction algorithm in assessing coronary artery calcification (CAC) degree and cardiovascular disease risk in patients receiving maintenance hemodialysis (MHD).

Methods In total, 181 patients receiving MHD who needed chest CT and coronary artery calcium score (CACS) scannings sequentially underwent non-ECG-triggered, automated tube voltage selection, high-pitch chest LDCT with a kV-independent reconstruction algorithm and ECG-triggered standard CACS scannings. Then, the image quality, radiation doses, Agatston scores (ASs), and cardiac risk classifications of the two scans were compared.

Results Of the 181 patients, 89, 83, and 9 were scanned at 100, 110, and 120 kV, respectively. Excluding those scanned at 120 kV, 172 patients were enrolled. Although the ASs of non-ECG-triggered LDCT were lower than those of the standard CACS, the agreement and correlation of ASs of the two scans were excellent, and both intraclass correlation coefficients (ICCs) and Pearson's correlation coefficients were > 0.96. Cardiac risk classifications did not significantly differ between the non-ECG-triggered LDCT and standard CACS ($\chi^2 = 3.933$, $P = 0.269$), and the agreement was excellent (weighted kappa value = 0.936; 95% confidence interval (CI): 0.903–0.970). The effective radiation doses of standard CACS and non-ECG-triggered chest LDCT scannings were 1.34 ± 0.74 and 1.04 ± 0.35 mSv, respectively.

Conclusions The non-ECG-triggered, automated tube voltage selection, high-pitch chest LDCT protocol with a kV-independent reconstruction algorithm can obtain chest scans and ASs simultaneously and significantly reduce patients' radiation exposure.

†Xiangming Wang and Ao Liu contributed equally to this work.

*Correspondence:
Li Yang
48000664@hebmu.edu.cn
Full list of author information is available at the end of the article

Keywords Coronary artery disease, Vascular calcification, Risk factors, Tomography, X-ray computed, Radiation dosage

Introduction

Maintenance hemodialysis (MHD) is a life-sustaining transitional treatment for patients with end-stage renal disease. Patients receiving MHD are often accompanied with risk factors for cardiovascular diseases, including hypertension, abnormal glucose and lipid metabolism, anemia, triglyceride–glucose index, and abnormal calcium and phosphorus metabolism [1, 2]. The incidence of cardiovascular disease in patients receiving MHD is 20–30 times higher than that in healthy individuals, and 50% of patients receiving MHD die of cardiovascular disease [3, 4]. Coronary artery calcification (CAC) is an early sign [5] and one of the important pathological changes of coronary atherosclerosis. Its incidence in patients receiving MHD is 2.5–5 times higher than that in healthy individuals [6, 7]. Agatston score (AS) is the most widely used method for quantifying the degree of CAC on the basis of computed tomography (CT) scans, which can effectively predict the risk of developing cardiovascular events and facilitate in preventing them [8–11]. However, AS requires a fixed attenuation threshold (130 Hounsfield units [HU]) to detect CAC using noncontrast CT with a fixed tube voltage of 120 kV and a slice thickness of 3 mm [12]. Notably, changes in scanning and reconstruction parameters can affect AS accuracy [13–15]. Therefore, the radiation dose has been maintained at high levels (1–1.5 mSv) [16, 17]. Accurately quantifying calcified plaque and assessing cardiac risk classification at the lowest possible radiation dose according to the "as low as reasonably achievable principle" proposed by the International Commission of Radiological Protection has always been a research interest.

A recently developed kV-independent reconstruction algorithm reduces the effect of tube voltage on AS, generating images at any tube voltage with HU values equivalent to 120 kV for bone and calcium; consequently, consistent AS at lower tube voltage without changing the attenuation threshold can be achieved [18–20]. To reduce the radiation dose further and the influence of cardiac motion on the display of coronary calcified plaques through non-ECG-triggered scans, this study aimed to simultaneously perform chest CT and coronary artery calcium score (CACS) scans by combining non-ECG-triggered, automated tube voltage selection, high-pitch low-dose CT (LDCT) and the kV-independent reconstruction algorithm. The AS and the cardiac risk classification obtained from the standard CACS scanning protocol were compared between the two scans to evaluate the feasibility and accuracy of non-ECG-triggered chest LDCT in assessing the degree of CAC and the risk of developing cardiovascular diseases in patients receiving MHD.

Materials and methods

Study population

This prospective, single-center study received approval from the Ethics Committee of the Fourth Hospital of Hebei Medical University and obtained written informed consent from all patients. Data from patients receiving MHD who underwent CACS scans in our hospital between June and September of 2022 were continuously collected. The inclusion criteria were as follows: ① received hemodialysis treatment; ② required to undergo chest CT and CACS scans simultaneously to meet the needs of clinical diagnosis and treatment. We excluded patients with a history of coronary artery stent implantation, coronary artery bypass grafting, or prosthetic heart valve replacement. In total, 181 patients met the above-mentioned criteria.

Sample size calculation

The sample size was calculated according to the minimum number of study participants required to assess the agreement between two diagnostic methods. For agreement studies evaluating diagnostic methods where the expected intraclass correlation coefficient (ICC)/kappa value is ≥ 0.80 with a desired 95% confidence interval (CI) of 0.1–0.2, the required sample size is approximately 150–200 cases [21]. Considering potential dropouts, we initially planned to enroll 200 patients. Ultimately, we completed data collection for 172 cases.

Acquisition protocols

We used a third-generation 192-slice dual-source CT scanner (SOMATOM Force; Siemens Healthineers, Forchheim, Germany). Each participant sequentially underwent non-ECG-triggered, automated tube voltage selection, high-pitch chest LDCT scans and ECG-triggered standard CACS scans. Table 1 presents the scan parameters. None of the patients took drugs for heart rate control before the scans.

Image quality

Observer 1 (YSC) with 3 years of experience in imaging diagnosis measured the HU values of the ascending aorta at the left main coronary artery (LMA) level.

Table 1 Parameters of the non-ECG-triggered chest LDCT and standard CACS scans

	Non-ECG-triggered Chest LDCT	Standard CACS
kV	CARE kV (Ref.kV110)	120 kV
mAs	CARE Dose 4D	CARE Dose 4D
Reference mAs	52 mAs	80 mAs
Pitch	3	0.15
Collimation	192 × 0.6 mm	192 × 0.6 mm
Rotation time	0.25 s	0.25 s
Reconstruction	FBP	FBP
Slice	3 mm	3 mm
Increment	1.5 mm	1.5 mm
Kernel	Sa36	Qr36
Scan area	thorax	heart
Scan time	0.5–0.7 s	6.05 s
SFOV	500 mm	500 mm
DFOV	heart 200 mm; thorax 350 mm	200 mm

The HU values' standard deviation ($SD_{ascending\ aorta}$) was used as image noise to calculate the signal-to-noise ratio (SNR) as follows: $SNR = CT_{ascending\ aorta} / SD_{ascending\ aorta}$. Furthermore, using the HU values of intrapericardial adipose tissue around the LMA at the same level, we calculated the contrast-to-noise ratio (CNR) as follows: $CNR = (CT_{ascending\ aorta} - CT_{intrapericardial\ adipose\ tissue}) / SD_{ascending\ aorta}$.

Coronary artery calcium scoring

Visual Score (VS)

Observer 1 and observer 2 (ML; with 15 years of experience in imaging diagnosis) visually evaluated non-ECG-triggered CACS scans according to the expert consensus "Coronary Artery Calcium Data and Reporting System (CAC-DRS)" developed by the Society of Cardiovascular Computed Tomography (SCCT) [22]. Inconsistencies between the observers' results were resolved by observer 3 (LY) with 20 years of experience in imaging diagnosis. Patients were stratified for cardiovascular risk according to the final results as follows: category 0, none (very low); category 1, mild (mildly increased); category 2, moderate (moderately increased); and category 3, severely (moderately-to-severely increased).

AS

Images were analyzed using semi-automatic CACS software (syngo.via, version VB10B, Calcium Scoring, Siemens Healthineers). To avoid memory bias, observer 1 randomly marked the calcified plaque areas of the LMA, left anterior descending artery (LAD), left circumflex artery (LCX), and right coronary artery (RCA) of the two scans. Then, observer 2 confirmed the marked areas. Any disagreements were resolved by observer 3. After marking, the software automatically identified continuous pixels with an area of at least 1.03 mm^2 and an attenuation threshold of 130 HU, followed by AS calculation. The cardiovascular risk of patients was stratified according to AS based on the CAC-DRS [22] as follows: category 0, 0 (very low); category 1, 1–99 (mildly increased); category 2, 100–299 (moderately increased); and category 3, ≥ 300 (moderately-to-severely increased). Figure 1 illustrates the study's flowchart.

Radiation dose

We recorded the volume CT dose index ($CTDI_{vol}$) and dose-length product (DLP) of the non-ECG-triggered chest LDCT and standard CACS scans. The effective radiation dose (ED) was calculated as follows: $ED = DLP \times k$, where k is a conversion factor of 0.014 mSv/(mGy.cm).

Statistical analysis

We used Statistical Package for the Social Sciences version 27.0 (IBM) for the statistical analysis. Normally distributed continuous variables, expressed as mean ± SD, were compared between two groups by using Student's *t*-test. The ICC was calculated to assess the agreement of the non-ECG-triggered coronary artery calcium VS obtained by observers 1 and 2. Furthermore, we conducted Bland–Altman analysis and calculated the ICCs to assess the agreement of AS between the two scans, as well as Pearson's correlation coefficients to examine the correlation between the two. We also employed the McNemar test and calculated the weighted kappa to compare the cardiovascular disease risk classification and to assess the agreement between the two scans, respectively. To evaluate the accuracy of cardiovascular risk stratification between patients with heart rates ≥ 80 and < 80 beats per minute (BPM), we utilized Fisher's exact test. Student's *t*-test and chi-square test were used to compare differences between correct and incorrect groups in the risk classification of non-ECG-triggered chest LDCT scans. The ICC or kappa values of ≤ 0.10, 0.11–0.40, 0.41–0.60, 0.61–0.80, and 0.81–1.00 indicate no, poor, general, moderate, and excellent agreement, respectively.

Results

Among the 181 patients, 89, 83, and 9 were scanned at 100, 110, and 120 kV, respectively. Excluding those scanned at a tube voltage of 120 kV, 172 patients were finally enrolled, comprising 113 men and 59 women. Their mean age range, weight, and body mass index (BMI) were 20–90 years (mean age: 57.12 ± 15.43 years), 63.22 ± 12.47 kg, and 22.77 ± 3.62 kg/m^2, respectively.

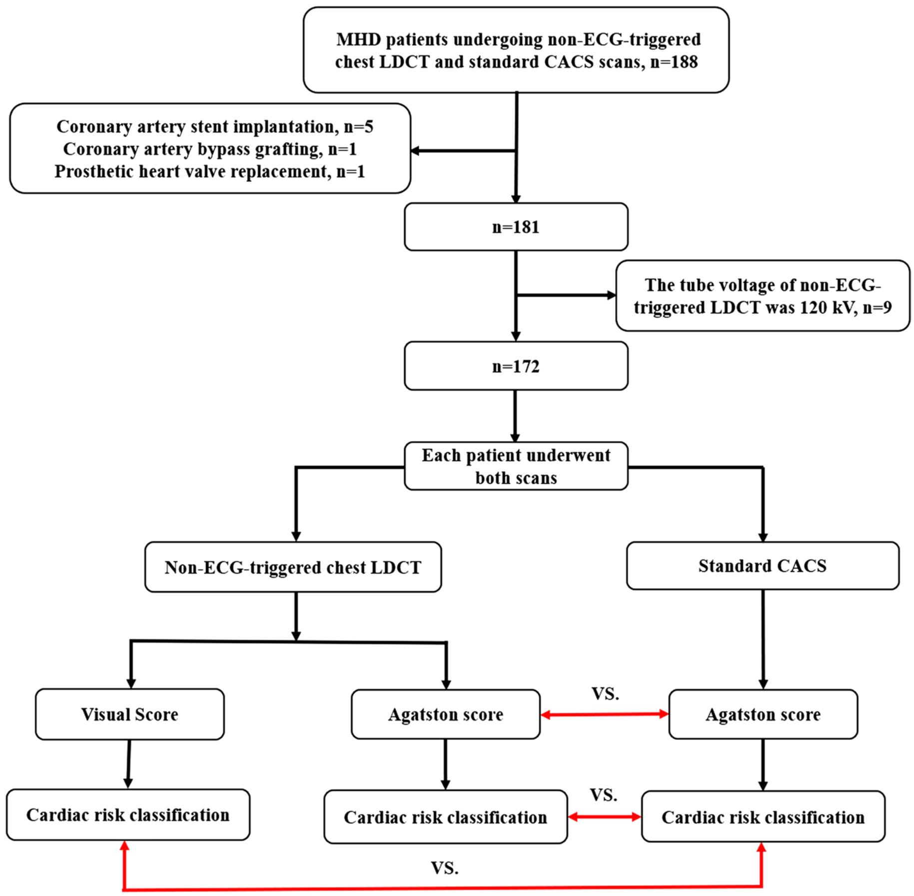

Fig. 1 Flowchart of this study

During the standard CACS scans, the mean heart rate was 72.07 ± 12.32 beats/min (Table 2).

Comparison of image quality and radiation dose between the two scans

The non-ECG-triggered chest LDCT scans had lower SD and higher SNR and CNR than the standard CACS scans ($P < 0.05$); however, the values of these scans were very close, and the image quality was equivalent. Notably, the EDs of the standard CACS and non-ECG-triggered chest LDCT scans were 1.34 ± 0.74 and 1.04 ± 0.35 mSv, respectively. Additionally, the mean ED and the $CTDI_{vol}$ were reduced by 21.77% and 59.93%, respectively (Table 3).

Non-ECG-triggered chest LDCT coronary artery calcium VS

Observers 1 and 2 had an excellent agreement on non-ECG-triggered chest LDCT VS (ICC = 0.944; 95% CI: 0.925–0.958) (Table 4). Meanwhile, cardiac risk classification significantly differed between the non-ECG-triggered VS and the standard CACS AS ($\chi^2 = 34.333$, $P < 0.001$; weighted kappa value = 0.813; 95% CI: 0.756–0.869). Considering the cardiac risk classification of

Table 2 Subgroup analysis for the different kV levels

kV	BMI (kg/m^2)	CTDI (mGy)	DLP (mGy × cm)	Effective Dose (mSv)
100 (*n* = 89)	21.57 ± 3.44	1.87 ± 0.89	61.43 ± 20.60	0.86 ± 0.29
110 (*n* = 83)	24.07 ± 3.36	2.67 ± 0.59	88.48 ± 20.84	1.24 ± 0.29
t value	− 4.815	− 6.863	− 8.556	− 8.556
P	< 0.001	< 0.001	< 0.001	< 0.001

Table 3 Image quality, radiation dose, and CAC degree between the two scans

		Standard CACS	Non-ECG-triggered Chest LDCT	T value	*P*	ICC (95%CI)	Correlation Coefficients	*P*
Image Quality	**SD $_{Ascending\ Aorta}$**	15.53 ± 2.85	14.92 ± 1.72	3.320	0.001			
	SNR	3.14 ± 0.67	3.29 ± 0.53	3.585	< 0.001			
	CNR	9.06 ± 1.80	9.35 ± 1.33	2.301	0.023			
Radiation dose	**$CTDI_{vol}$ (mGy)**	5.64 ± 2.81	2.26 ± 0.86	16.730	< 0.001			
	ED (mSv)	1.34 ± 0.74	1.04 ± 0.35	5.378	< 0.001			
Calcified vessels	**N**	2.45 ± 1.33	2.44 ± 1.34	1.135	0.258	0.989(0.985–0.992)	0.989	< 0.001
ASs	**LMA**	47.03 ± 125.88	42.92 ± 114.71	2.259	0.025	0.980(0.973–0.985)	0.985	< 0.001
	LAD	325.24 ± 419.46	307.31 ± 415.77	4.043	< 0.001	0.990(0.987–0.993)	0.990	< 0.001
	LCX	142.76 ± 360.04	136.77 ± 367.03	0.852	0.396	0.968(0.957–0.976)	0.968	< 0.001
	RCA	286.54 ± 556.02	252.90 ± 526.27	5.427	< 0.001	0.989(0.985–0.992)	0.990	< 0.001
	Total	801.56 ± 1129.60	739.90 ± 1098.38	5.919	< 0.001	0.992(0.990–0.994)	0.993	< 0.001

Table 4 Agreement between the two observers' non-ECG-triggered chest LDCT VS

Observer 1	Observer 2				
	Category 0	Category 1	Category 2	Category 3	Total
Category 0	27	0	0	0	27
Category 1	0	17	6	0	23
Category 2	0	1	48	2	51
Category 3	0	0	13	58	71
Total	27	18	67	60	172

standard CACS as the gold standard, the accuracy of cardiac risk classification of non-ECG-triggered VS was 77.91% (134/172). Additionally, 38 patients were reclassified to another risk category, but all were adjacent-level reclassifications, with no cross-level reclassifications. Among them, 27 were underestimated, 11 were overestimated, and 4 were false-negative (Fig. 2).

Non-ECG-triggered chest LDCT coronary artery calcium AS

The number of calcified vessels did not significantly differ between the non-ECG-triggered LDCT and standard CACS scans, with excellent agreement ($P > 0.05$; ICC = 0.989; 95% CI: 0.985–0.992). Except for LCX, the ASs of the LMA, LAD, and RCA, as well as the total scores, obtained from the two scans showed significant differences (all $P < 0.05$). Bland–Altman plots revealed a slight difference in ASs between the two scans (Fig. 3). ASs obtained from non-ECG-triggered LDCT were lower than those obtained from the standard CACS, with a mean difference of 61.67 in the total scores. The largest mean difference among the four vessels was noted in RCA (33.64). However, the agreement and correlation of ASs obtained from the two scans were excellent, and both ICCs and Pearson's correlation coefficients were > 0.96. Cardiac risk classification did not significantly differ between such scans ($\chi^2 = 3.933$, $P = 0.269$), demonstrating excellent agreement (weighted kappa value = 0.936; 95% CI: 0.903–0.970). The accuracy of cardiac risk classification of the non-ECG-triggered AS was 92.44% (159/172), considering the cardiac risk classification of standard CACS as the gold standard. This risk stratification was more accurate in patients with heart rates < 80 BPM (93.9%) than those with heart rates ≥ 80 BPM (87.8%), although the difference was not statistically significant ($P = 0.194$). Additionally, 13 patients were reclassified to another risk category, but all were adjacent-level reclassifications, with no cross-level reclassifications. Among them, 10 were underestimated, 3 were overestimated, 2 were false-negative, and 1 was false-positive (Fig. 2). The ASs of the correct group in the non-ECG-triggered LDCT were higher than those of the incorrect group ($P < 0.05$), with no significant difference in BMI, heart rate, scan voltage, and image noise ($P > 0.05$; Table 5).

Other abnormal signs found in non-ECG-triggered chest LDCT scans

Other abnormal signs found in non-ECG-triggered chest LDCT scans were pulmonary inflammation, pulmonary nodules, enlarged mediastinal lymph nodes, and gallstones in 58, 140, 5, and 9 patients, respectively (Fig. 4).

Discussion

This pilot study demonstrated that chest scans and AS can be obtained simultaneously by combining non-ECG-triggered, automated tube voltage selection, high-pitch

Standard CACS AS

Non-ECG-triggered Chest LDCT		Category 0	Category 1	Category 2	Category 3	Total
VS	Category 0	23	4	0	0	27
	Category 1	0	20	1	0	21
	Category 2	0	11	24	22	57
	Category 3	0	0	0	67	67
	Total	23	35	25	89	172
AS	Category 0	22	2	0	0	24
	Category 1	1	32	4	0	37
	Category 2	0	1	20	4	25
	Category 3	0	0	1	85	86
	Total	23	35	25	89	172

Fig. 2 Agreement of cardiac risk classification obtained from the two scans

chest LDCT and a kV-independent reconstruction algorithm in patients receiving MHD. This protocol can accurately demonstrate the degree of CAC, maintain the overall cardiac risk classification, implement one-stop scanning of the chest and reveal AS, and significantly reduce the radiation exposure of patients, thereby potentially useful for clinical application.

The AS depends on the tube voltage, and the CACS scanning protocol of < 120 kV can increase the CT attenuation value of calcification, resulting in AS overestimation [23–25]. Some studies adjusted the threshold to obtain AS with excellent agreement between reduced voltage scans and standard CACS scans [13, 23, 26]. The metallic components of coronary stents, surgical bypass grafts, and mechanical heart valves can affect calcified plaque identification and measurement; therefore, we excluded patients with these conditions. The kV-independent reconstruction algorithm (Sa36) uses a voltage-dependent lookup table based on raw data for the image reconstruction of acquired noncontrast CT. It can reproduce 120 kV-equivalent images for a range of tube voltage settings without the need for changing the calcium threshold. Vingiani et al. [18] found that combining automated tube voltage selection, ECG-triggered, and kV-independent reconstruction algorithm yielded an excellent correlation of AS compared with using the standard 120-kVp acquisition protocol. Our study revealed that the ASs derived from non-ECG-triggered chest LDCT scans were slightly lower than those derived from standard CACS scans, possibly related to the use of non-ECG-triggered scans. Additionally, non-ECG-triggered scans can help reduce the radiation dose significantly [27, 28]. A study demonstrated an excellent correlation between the ASs derived from the non-ECG-triggered and standard CACS scans and excellent agreement in the cardiac risk classification derived from these two scans [27]. However, non-ECG-triggered scans cannot suppress cardiac motion artifacts, affecting the accuracy of AS. The RCA exhibits the highest degree of systolic–diastolic motion of heart vessels and produces the most severe motion artifacts. In our study, the difference in the total AS was mainly caused by differences in AS of the RCA (33.64/61.67, 54.55%), consistent with the results reported by Hutt et al. [28]. In a previous study, AS had limited reproducibility, and CT scan machines made by different manufacturing companies produced substantially different ASs [29]. Moreover, ASs even differed between two scannings performed using the same scanner and protocol [30, 31]. This study used a high-pitch scan to reduce the radiation dose [23, 32] while shortening the scanning time, thereby relatively decreasing the impact of cardiac motion artifacts on AS. The two scans had an excellent agreement in cardiac risk classification (weighted kappa value = 0.936; 95% CI: 0.903–0.970), and the accuracy of risk classification by non-ECG-triggered chest LDCT was 92.44%, which is similar to those reported in previous studies [33, 34]. Lower heart rates are associated with reduced coronary motion artifacts. Nonetheless, our study demonstrated that the accuracy of risk stratification did not significantly differ between

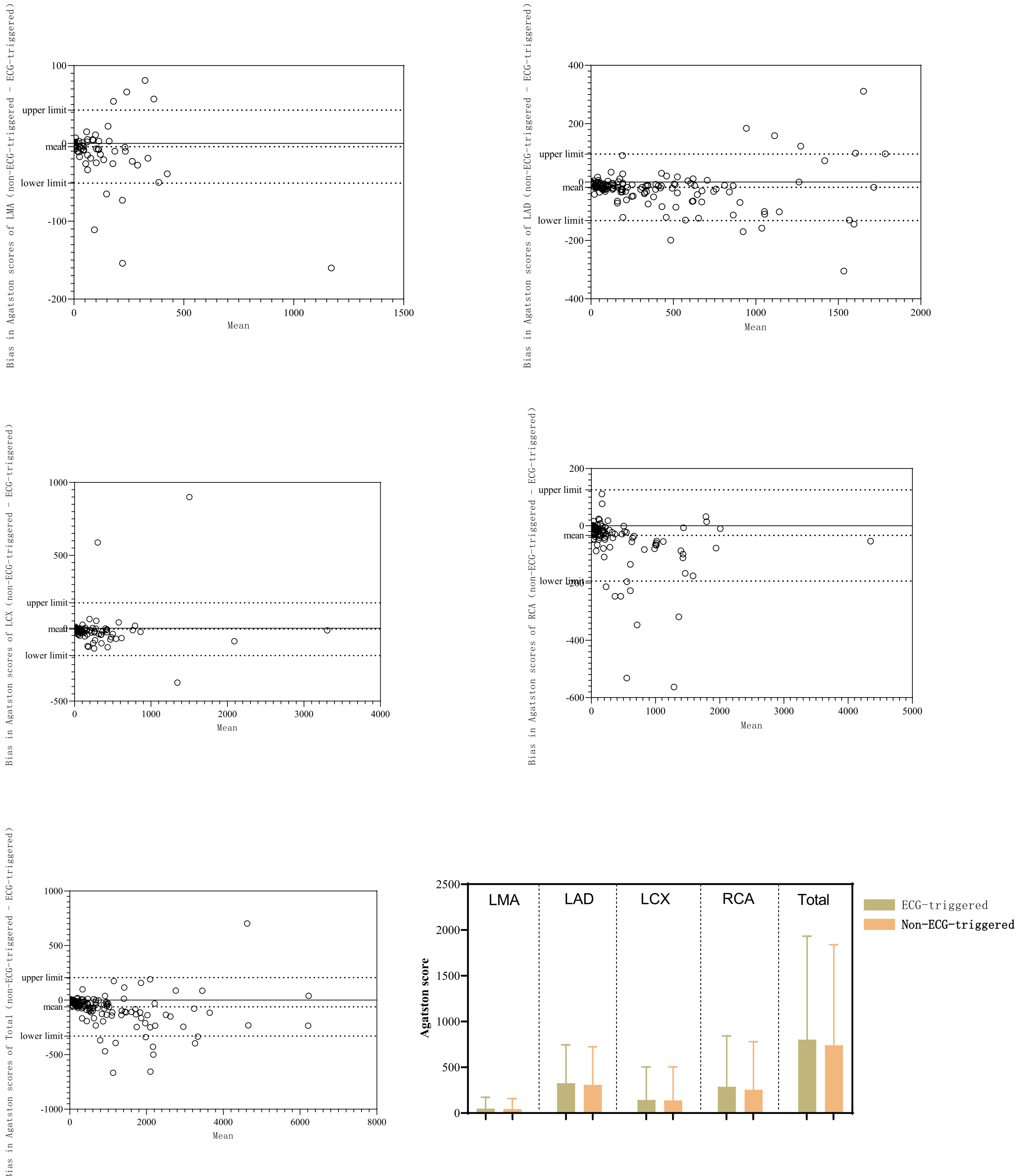

Fig. 3 Bland–Altman plots and column chart of Agatston scores obtained from the standard CACS and non-ECG-triggered chest LDCT scans. Bland–Altman plots revealed a slight difference in ASs between the two scans. The mean differences in the scores for LMA, LAD, LCX, and RCA were 4.1, 17.9, 6.0, and 33.6, respectively, with 95% limits of agreement of − 51.0 to + 42.7, − 131.9 to + 96.1, − 186.7 to + 174.8, and − 193.0 to + 125.7, respectively. The total mean difference was 61.7, with a 95% limit of agreement of − 329.5 to + 206.2

Table 5 Factors affecting the accuracy of cardiac risk classification of non-ECG-triggered LDCT AS

Cardiac Risk Classification of Non-ECG-triggered LDCT AS	BMI	Heart Rate	Scans Voltage		Image Noise	Standard CACS AS
			100 kV	110 kV		
Incorrect Group	24.39 ± 4.01	76.62 ± 15.13	5(38.5)	8(61.5)	14.62 ± 1.62	176.46 ± 140.41
Correct Group	22.64 ± 3.56	71.70 ± 12.04	84(52.8)	75(47.2)	14.95 ± 1.73	852.67 ± 1159.61
t/χ^2 value	1.685	1.387	0.994		− 0.652	− 6.771
P	0.094	0.167	0.319		0.515	< 0.001

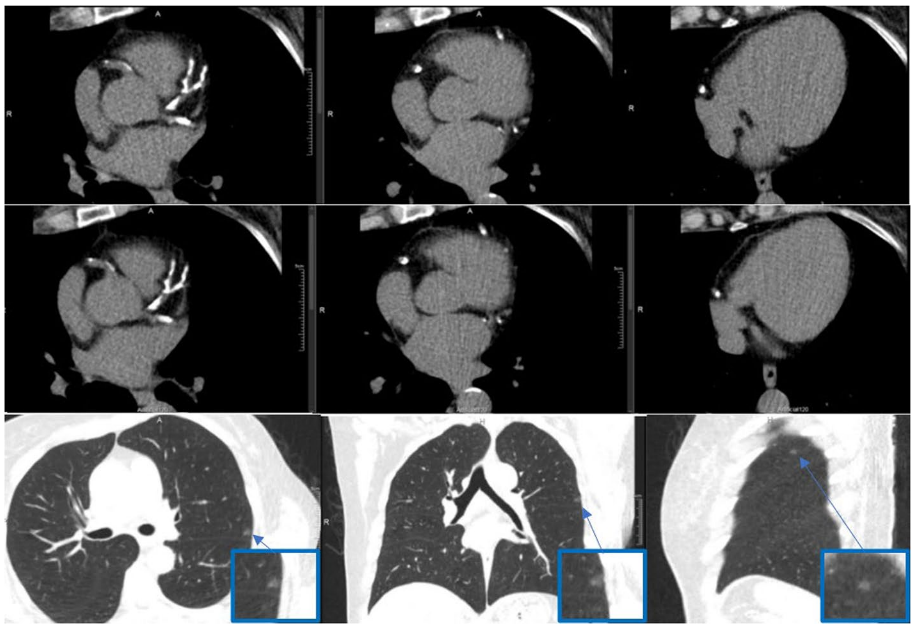

Fig. 4 Top row: cardiac CT scan of a standard 120 kV protocol. Middle row: cardiac CT scan acquired using non-ECG-triggered chest LDCT reconstructed with kV-independent reconstruction algorithm. Bottom row: non-ECG-triggered chest LDCT scan (lung window)

patients with heart rates < 80 and ≥ 80 BPM, possibly because of the use of high-pitch scanning, which shortens scan duration and minimizes the influence of coronary motion artifacts in patients with higher heart rates. Patients in the incorrect group had lower ASs than those in the correct group, likely related to low-risk stratification requiring higher AS accuracy. The long-term clinical implications of this method in assessing the risk of developing cardiovascular diseases in patients receiving MHD require further investigation.

This study combined non-ECG-triggered, automated tube voltage selection, and high-pitch scans. The $CTDI_{vol}$ was reduced by 59.93% compared with the standard CACS scans, and chest scans and ASs could be obtained simultaneously. This protocol significantly reduced the radiation exposure of patients and maintained the overall cardiac risk classification. Moreover, all image noises met the standard recommended by the SCCT, where the image noise of CACS scans should be < 23 HU [17].

Additionally, the guidelines issued by the SCCT and the Society of Thoracic Radiology recommend visual estimation of CAC and AS on noncardiac-gated chest CT images [22]. In our study, the visual estimation of CAC was less accurate (77.91%) and poorly sensitive and could only roughly evaluate the degree of CAC despite a good interobserver agreement.

Our study has the following limitations. First, this was a single-center study with a relatively low number of patients and a small range of tube voltages (100 and 110 kV only). Second, it only focused on the effect of the non-ECG-triggered LDCT protocol on the AS and not on the volume and mass scores of CAC. Third, our findings may not be generalizable or adjustable to other CT system manufacturers, considering that the image datasets were postprocessed using a manufacturer-specific kV-independent reconstruction algorithm. Finally, AS evaluation relies on manual marking of the calcified plaque areas and radiologists' judgment, thereby likely influenced by subjective factors. However, with the application of AI technology in cardiovascular diseases, the stability, sensitivity, and accuracy of detecting calcified plaques can be enhanced [35].

Conclusion

Combining the non-ECG-triggered, automated tube voltage selection, high-pitch chest LDCT protocol and a kV-independent reconstruction algorithm enables one-stop scanning of the chest and AS, accurately demonstrates the degree of CAC, maintains the overall cardiac risk classification, and significantly reduces the radiation exposure of patients.

Abbreviations

ECG	Electrocardiogram
LDCT	Low-dose computed tomography
CAC	Coronary artery calcification
MHD	Maintenance hemodialysis
CACS	Coronary artery calcium score
AS	Agatston score
ICC	Intraclass correlation coefficient
CI	Confidence interval
HU	Hounsfield units
SNR	Signal-to-noise ratio
SD	Standard deviation
CNR	Contrast-to-noise ratio
VS	Visual score
CAC-DRS	Coronary Artery Calcium Data and Reporting System
SCCT	Cardiovascular Computed Tomography
LMA	Left main coronary artery
LAD	Left anterior descending artery
LCX	Left circumflex artery
RCA	Right coronary artery
$CTDI_{vol}$	Volume CT dose index
DLP	Dose-length product
ED	Effective radiation dose
BPM	Beats per minute
BMI	Body mass index

Authors' contributions

All authors contributed to the study conception and design. Data collection was performed by LY, YC, ML, JL and YD. Data analysis was performed by YZ and XY. The first draft of the manuscript was written by XW and AL. The manuscript was reviewed and edited by LY and all authors commented on previous versions of the manuscript. All authors read and approved the final manuscript.

Funding

The authors declare that no funds, grants, or other support were received during the preparation of this manuscript.

Data availability

The datasets used and/or analysed during the current study are available from the corresponding author on reasonable request.

Declarations

Ethics approval and consent to participate

This study was approved by the Ethics Committee of the Fourth Hospital of Hebei Medical University, and the ethics approval number was 2023KS130. Written informed consent was obtained from all patients.

Consent for publication

Not applicable.

Competing interests

The authors declare no competing interests.

Author details

[1]Department of Computed Tomography and Magnetic Resonance, Fourth Hospital of Hebei Medical University, Shijiazhuang, China. [2]School of Mathematics and Science, Hebei GEO University, Shijiazhuang, China. [3]CT Collaboration, Siemens Healthineers Ltd, Beijing, China.

Received: 17 April 2024 Accepted: 14 January 2025
Published online: 24 January 2025

References

1. Boronat M, Santana Á, Bosch E, Lorenzo D, Riaño M, García-Cantón C. Relationship between anemia and serum concentrations of calcium and phosphorus in advanced non-dialysis-dependent chronic kidney disease. Nephron. 2017;135(2):97–104. https://doi.org/10.1159/000450892.
2. Hayıroğlu Mİ, Çınar T, Çiçek V, Palice A, Ayhan G, Tekkeşin Aİ. The triglyceride-glucose index can predict long-term major adverse cardiovascular events in turkish patients with high cardiovascular risk. Journal of lipid and atherosclerosis. 2022;11(3):280–7. https://doi.org/10.12997/jla.2022.11.3.280.
3. Ishii H, Takahashi H, Ito Y, Aoyama T, Kamoi D, Sakakibara T, Umemoto N, Kumada Y, Suzuki S, Murohara T. The association of ankle brachial index, protein-energy wasting, and inflammation status with cardiovascular mortality in patients on chronic hemodialysis. Nutrients. 2017;9(4):416. https://doi.org/10.3390/nu9040416.
4. Xiong Y, Li J, Sun S, Han M, Liao R, Li Y, Wang L, Lin L, Liu Q, Su B. Association of mineral content outside of bone with coronary artery calcium and 1-year cardiovascular prognosis in maintenance hemodialysis patients. Artif Organs. 2019;43(10):988–1001. https://doi.org/10.1111/aor.13461.
5. Osawa K, Nakanishi R, Budoff M. Coronary artery calcification global heart. 2016;11(3):287–93. https://doi.org/10.1016/j.gheart.2016.08.001.
6. Samaan F, Carvalho AB, Pillar R, Rocha LA, Cassiolato JL, Cuppari L, Canziani MEF. The effect of long-term cholecalciferol supplementation on vascular calcification in chronic kidney disease patients with hypovitaminosis D. Journal of renal nutrition : the official journal of the Council on Renal Nutrition of the National Kidney Foundation. 2019;29(5):407–15. https://doi.org/10.1053/j.jrn.2018.12.002.
7. Carlsen RK, Winther S, Peters CD, Laugesen E, Khatir DS, Bøtker HE, Bøttcher M, Ivarsen P, Svensson M, Buus NH. Aortic calcification affects noninvasive estimates of central blood pressure in patients with severe chronic kidney disease. Kidney Blood Press Res. 2019;44(4):704–14. https://doi.org/10.1159/000501226.
8. Peng AW, Mirbolouk M, Orimoloye OA, Osei AD, Dardari Z, Dzaye O, Budoff MJ, Shaw L, Miedema MD, Rumberger J, Berman DS, Rozanski A, Al-Mallah MH, Nasir K, Blaha MJ. Long-term all-cause and cause-specific mortality in asymptomatic patients with CAC ≥1,000: results from the CAC consortium. JACC Cardiovasc Imaging. 2020;13(1 Pt 1):83–93. https://doi.org/10.1016/j.jcmg.2019.02.005.
9. Silverman MG, Blaha MJ, Krumholz HM, Budoff MJ, Blankstein R, Sibley CT, Agatston A, Blumenthal RS, Nasir K. Impact of coronary artery calcium on coronary heart disease events in individuals at the extremes of traditional risk factor burden: the Multi-Ethnic Study of Atherosclerosis. Eur Heart J. 2014;35(33):2232–41. https://doi.org/10.1093/eurheartj/eht508.
10. Hecht HS. Coronary artery calcium scanning: past, present, and future. JACC Cardiovasc Imaging. 2015;8(5):579–96. https://doi.org/10.1016/j.jcmg.2015.02.006.
11. Hecht H, Blaha MJ, Berman DS, Nasir K, Budoff M, Leipsic J, Blankstein R, Narula J, Rumberger J, Shaw LJ. Clinical indications for coronary artery calcium scoring in asymptomatic patients: Expert consensus statement from the Society of Cardiovascular Computed Tomography. J Cardiovasc Comput Tomogr. 2017;11(2):157–68. https://doi.org/10.1016/j.jcct.2017.02.010.
12. Agatston AS, Janowitz WR, Hildner FJ, Zusmer NR, Viamonte M Jr, Detrano R. Quantification of coronary artery calcium using ultrafast computed tomography. J Am Coll Cardiol. 1990;15(4):827–32. https://doi.org/10.1016/0735-1097(90)90282-t.

13. Vonder M, van der Werf NR, Leiner T, Greuter MJW, Fleischmann D, Vliegenthart R, Oudkerk M, Willemink MJ. The impact of dose reduction on the quantification of coronary artery calcifications and risk categorization: A systematic review. J Cardiovasc Comput Tomogr. 2018;12(5):352–63. https://doi.org/10.1016/j.jcct.2018.06.001.
14. Tesche C, De Cecco CN, Schoepf UJ, Duguay TM, Albrecht MH, Caruso D, Varga-Szemes A, Lesslie VW, Ebersberger U, Canstein C, Thilo C, Hoffmann E, Allmendinger T, Nance JW. Iterative beam-hardening correction with advanced modeled iterative reconstruction in low voltage CT coronary calcium scoring with tin filtration: Impact on coronary artery calcium quantification and image quality. J Cardiovasc Comput Tomogr. 2017;11(5):354–9. https://doi.org/10.1016/j.jcct.2017.07.003.
15. Willemink MJ, Takx RA, de Jong PA, Budde RP, Bleys RL, Das M, Wildberger JE, Prokop M, Buls N, de Mey J, Schilham AM, Leiner T. The impact of CT radiation dose reduction and iterative reconstruction algorithms from four different vendors on coronary calcium scoring. Eur Radiol. 2014;24(9):2201–12. https://doi.org/10.1007/s00330-014-3217-7.
16. Patel AA, Fine J, Naghavi M, Budoff MJ. Radiation exposure and coronary artery calcium scans in the society for heart attack prevention and eradication cohort. Int J Cardiovasc Imaging. 2019;35(1):179–83. https://doi.org/10.1007/s10554-018-1431-0.
17. Voros, S., Rivera, J. J., Berman, D. S., Blankstein, R., Budoff, M. J., Cury, R. C., Desai, M. Y., Dey, D., Halliburton, S. S., Hecht, H. S., Nasir, K., Santos, R. D., Shapiro, M. D., Taylor, A. J., Valeti, U. S., Young, P. M., Weissman, G., Society for Atherosclerosis Imaging and Prevention Tomographic Imaging and Prevention Councils, & Society of Cardiovascular Computed Tomography. Guideline for minimizing radiation exposure during acquisition of coronary artery calcium scans with the use of multidetector computed tomography: a report by the society for atherosclerosis imaging and prevention tomographic imaging and prevention councils in collaboration with the society of cardiovascular computed tomography. J Cardiovasc Comput Tomogr. 2011;5(2):75–83. https://doi.org/10.1016/j.jcct.2011.01.003.
18. Vingiani V, Abadia AF, Schoepf UJ, Fischer AM, Varga-Szemes A, Sahbaee P, Allmendinger T, Giovagnoli DA, Hudson HT, Marano R, Tinnefeld FC, Martin SS. Individualized coronary calcium scoring at any tube voltage using a kV-independent reconstruction algorithm. Eur Radiol. 2020;30(11):5834–40. https://doi.org/10.1007/s00330-020-06951-1.
19. Tao S, Sheedy E, Bruesewitz M, Weber N, Williams K, Halaweish A, Schmidt B, Williamson E, McCollough C, Leng S. Technical Note: kV-independent coronary calcium scoring: A phantom evaluation of score accuracy and potential radiation dose reduction. Med Phys. 2021;48(3):1307–14. https://doi.org/10.1002/mp.14663.
20. Booij R, van der Werf NR, Budde RPJ, Bos D, van Straten M. Dose reduction for CT coronary calcium scoring with a calcium-aware image reconstruction technique: a phantom study. Eur Radiol. 2020;30(6):3346–55. https://doi.org/10.1007/s00330-020-06709-9.
21. Bourredjem A, Cardot H, Devilliers H. Asymptotic confidence interval, sample size formulas and comparison test for the agreement intra-class correlation coefficient in inter-rater reliability studies. Stat Med. 2024;43(27):5060–76. https://doi.org/10.1002/sim.10217.
22. Hecht HS, Blaha MJ, Kazerooni EA, Cury RC, Budoff M, Leipsic J, Shaw L. CAC-DRS: Coronary Artery Calcium Data and Reporting System An expert consensus document of the Society of Cardiovascular Computed Tomography (SCCT). J Cardiovasc Comput Tomogr. 2018;12(3):185–91. https://doi.org/10.1016/j.jcct.2018.03.008.
23. Marwan M, Mettin C, Pflederer T, Seltmann M, Schuhbäck A, Muschiol G, Ropers D, Daniel WG, Achenbach S. Very low-dose coronary artery calcium scanning with high-pitch spiral acquisition mode: comparison between 120-kV and 100-kV tube voltage protocols. J Cardiovasc Comput Tomogr. 2013;7(1):32–8. https://doi.org/10.1016/j.jcct.2012.11.004.
24. Apfaltrer G, Albrecht MH, Schoepf UJ, Duguay TM, De Cecco CN, Nance JW, De Santis D, Apfaltrer P, Eid MH, Eason CD, Thompson ZM, Bauer MJ, Varga-Szemes A, Jacobs BE, Sorantin E, Tesche C. High-pitch low-voltage CT coronary artery calcium scoring with tin filtration: accuracy and radiation dose reduction. Eur Radiol. 2018;28(7):3097–104. https://doi.org/10.1007/s00330-017-5249-2.
25. Tesche C, De Cecco CN, Vliegenthart R, Albrecht MH, Varga-Szemes A, Duguay TM, Ebersberger U, Bayer RR 2nd, Canstein C, Schmidt B, Allmendinger T, Litwin SE, Morris PB, Flohr TG, Hoffmann E, Schoepf UJ. Accuracy and radiation dose reduction using low-voltage computed tomography coronary artery calcium scoring with tin filtration. Am J Cardiol. 2017;119(4):675–80. https://doi.org/10.1016/j.amjcard.2016.10.051.
26. Gräni C, Vontobel J, Benz DC, Bacanovic S, Giannopoulos AA, Messerli M, Grossmann M, Gebhard C, Pazhenkottil AP, Gaemperli O, Kaufmann PA, Buechel RR. Ultra-low-dose coronary artery calcium scoring using novel scoring thresholds for low tube voltage protocols-a pilot study. Eur Heart J Cardiovasc Imaging. 2018;19(12):1362–71. https://doi.org/10.1093/ehjci/jey019.
27. Kim YK, Sung YM, Cho SH, Park YN, Choi HY. Reliability analysis of visual ranking of coronary artery calcification on low-dose CT of the thorax for lung cancer screening: comparison with ECG-gated calcium scoring CT. Int J Cardiovasc Imaging. 2014;30(Suppl 2):81–7. https://doi.org/10.1007/s10554-014-0507-8.
28. Hutt A, Duhamel A, Deken V, Faivre JB, Molinari F, Remy J, Remy-Jardin M. Coronary calcium screening with dual-source CT: reliability of ungated, high-pitch chest CT in comparison with dedicated calcium-scoring CT. Eur Radiol. 2016;26(6):1521–8. https://doi.org/10.1007/s00330-015-3978-7.
29. Willemink MJ, Vliegenthart R, Takx RA, Leiner T, Budde RP, Bleys RL, Das M, Wildberger JE, Prokop M, Buls N, de Mey J, Schilham AM, de Jong PA. Coronary artery calcification scoring with state-of-the-art CT scanners from different vendors has substantial effect on risk classification. Radiology. 2014;273(3):695–702. https://doi.org/10.1148/radiol.14140066.
30. Detrano RC, Anderson M, Nelson J, Wong ND, Carr JJ, McNitt-Gray M, Bild DE. Coronary calcium measurements: effect of CT scanner type and calcium measure on rescan reproducibility–MESA study. Radiology. 2005;236(2):477–84. https://doi.org/10.1148/radiol.2362040513.
31. Rutten A, Isgum I, Prokop M. Coronary calcification: effect of small variation of scan starting position on Agatston, volume, and mass scores. Radiology. 2008;246(1):90–8. https://doi.org/10.1148/radiol.2461070006.
32. McQuiston AD, Muscogiuri G, Schoepf UJ, Meinel FG, Canstein C, Varga-Szemes A, Cannao' PM, Wichmann JL, Allmendinger T, Vliegenthart R, De Cecco CN. Approaches to ultra-low radiation dose coronary artery calcium scoring based on 3rd generation dual-source CT: A phantom study. Eur J Radiol. 2016;85(1):39–47. https://doi.org/10.1016/j.ejrad.2015.10.023.
33. Jubran A, Mastrodicasa D, van Praagh GD, Willemink MJ, Kino A, Wang J, Fleischmann D, Nieman K. Low-dose coronary calcium scoring CT using a dedicated reconstruction filter for kV-independent calcium measurements. Eur Radiol. 2022;32(6):4225–33. https://doi.org/10.1007/s00330-021-08451-2.
34. Vingiani V, Abadia AF, Schoepf UJ, Fischer AM, Varga-Szemes A, Sahbaee P, Allmendinger T, Tesche C, Griffith LP, Marano R, Martin SS. Low-kV coronary artery calcium scoring with tin filtration using a kV-independent reconstruction algorithm. J Cardiovasc Comput Tomogr. 2020;14(3):246–50. https://doi.org/10.1016/j.jcct.2019.11.006.
35. Hayıroğlu Mİ, Altay S. The role of artificial intelligence in coronary artery disease and atrial fibrillation. Balkan Med J. 2023;40(3):151–2. https://doi.org/10.4274/balkanmedj.galenos.2023.06042023.

Publisher's Note